Filter-Based perturbation Control of low-Frequency Oscillation in Voltage-Mode H-Bridge DC-AC Inverter

Weiguo Lu [1*], Naikuan Zhao [1], Junke Wu [1], Abdelali El Aroudi[2], Luowei Zhou [1]

1 State Key Laboratory of Power Transmission Equipment & System Security and New Technology, Chongqing University, Chongqing 40044, P.R. China

2 Departament d'Enginyeria Electrònica, Elèctrica i Automàtica, Universitat Rovira i Virgili Tarragona, Tarragona 43007, Spain

SUMMARY

This paper presents a new additional perturbation control method for suppressing low-frequency oscillation in voltage-mode H-bridge DC-AC inverter. The stability boundary of the H-bridge inverter is investigated from its small-signal averaged model. High input voltage and light load would cause low-frequency oscillation in this system. To this end, a filter-based perturbation control (FBPC) is proposed for eliminating this oscillation, by using an analog filter to extract the unexpected signal and applying it to the control loop. Theoretical results show a larger stability range of the controlled system with the proposed FBPC. The simulation and experiment results show that the proposed controller can control the low-frequency oscillation in H-bridge DC-AC inverter well.

Keywords: H-bridge inverter, low-frequency oscillation, Filter-based perturbation control, Voltage mode.

*Correspondence to: Weiguo Lu, School of Electrical Engineering, Chongqing University, Chongqing 400044, P.R. China

E-mail address: luweiguo@cqu.edu.cn

1. INTRODUCTION

The inverter is widely used in electrical industry, which converters direct current (DC) into alternating current (AC), such as the grid inverter [1], uninterrupted power supply (UPS) [2] and so on. It outputs an expected low-frequency power signal by applying high-frequency switching signal to tracking a low-frequency reference. Therefore, the high-frequency instabilities in switching-ripple level and the low-frequency oscillation in reference-frequency level may occur in the inverter [3-6]. Period doubling bifurcation [7-8] and chaos [9-11] are the typical high-frequency instabilities and scholars have explored some strategies to control these high-frequency instabilities. Time-delayed feedback control (TDFC)[12] is effective way to stabilize the unstable periods in nonlinear system and it has been studied in inverters [13-15]. However, it is not a suitable method due to its difficult implementation with analog circuits. The low-frequency instability, known as low-frequency oscillation [16-18] in engineering can be analyzed by averaged model. It is called Hopf bifurcation from the dynamic perspective [5],[19]. As for the low-frequency oscillation, we can regulate the system parameters to avoid it. However, in this way it would reduce the system stability range. Up to now, few researchers explored the control method to suppress the low-frequency oscillation. As for the periodic instabilities in nonlinear system, we can apply a periodic perturbation signal to suppressing these instabilities. In our previous studies [20-21], we proposed a filter-based perturbation method to control of chaos in voltage-mode Buck DC-DC converter well, by using an analog filter to extract the unexpected signal and applying it to the control loop. In this paper, we will apply a filter-based perturbation control (FBPC) to eliminate the low-frequency oscillation in voltage-mode single-phase H-bridge DC-AC inverter.

The paper is organized as follows. Section 2 presents stability analysis by using the system average model. The proposed filter-based perturbation control (FBPC) is given in Section 3. Section 4 shows the simulation and experiment results and some conclusions are drawn in Section 5.

2. SYSTEM MODELING AND STABILITY ANALYSIS

Detailed analysis of low-frequency oscillation in the voltage-mode H-bridge DC-AC inverter has been reported in [5]. The oscillation frequency is higher than the frequency of reference voltage, but much lower than the switching frequency [3]. Therefore, this phenomenon can be predicted with the system averaged model. **Figure 1**(a) shows the schematic diagram of a voltage-mode single-phase H-bridge DC-AC inverter, where v_o is the output voltage, v_g is the DC input voltage with its average value V_g, v_d is the output voltage of the inverter bridge and v_{ref} is the sinusoid reference voltage. The inductor current and capacitor voltage are marked as i_L and v_C, respectively. The compensator is applied with a PI controller.

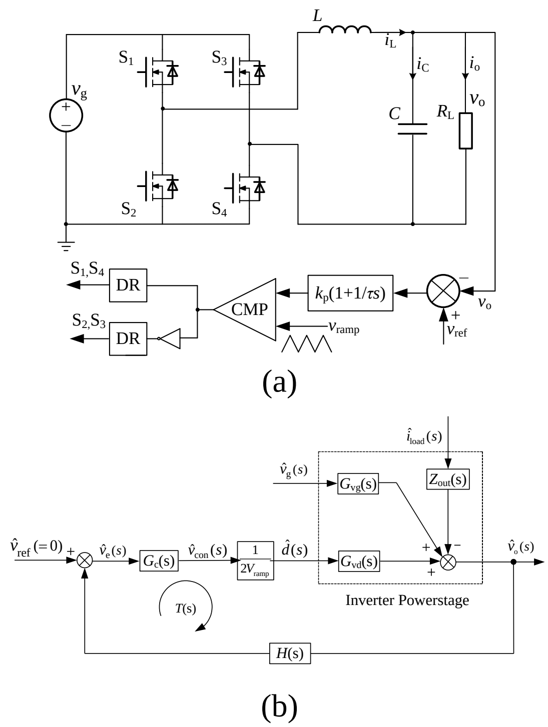

Figure 1. The voltage-mode single-phase H-bridge DC-AC inverter, (a) The power-stage and control circuits, (b) system block diagram

In the system block diagram **Figure 1(b)**, $G_{vd}(s)$ is the control-to-output transfer function, $G_{vg}(s)$ is the line-to-output transfer function, $Z_{out}(s)$ is the output impedance and $G_c(s)$ is the transfer function of the compensator, defined as $k_p(1+1/\tau s)$. Here, the expression of $G_{vd}(s)$ is

$$G_{vd}(s) = \frac{2v_g}{LCs^2 + (L/R)s + 1} \qquad (1)$$

The system stability can be investigated by the following closed-loop transfer function $F(s)$,

$$F(s) = \frac{1}{1+T(s)} \qquad (2)$$

where, $T(s)$ is the system loop gain,

$$T(s) = \frac{H}{V_{ramp}} G_{vd}(s) G_c(s) \qquad (3)$$

The characteristic polynomial equation is,

$$1+T(s)=s^3+a_2s^2+a_1s+a_0=0 \qquad (4)$$

where,

$$a_0=\frac{k_{\mathrm{p}}V_{\mathrm{g}}}{LC\tau V_{\mathrm{ramp}}}, \quad a_1=\frac{1}{LC}\left(1+\frac{k_{\mathrm{p}}V_{\mathrm{g}}}{V_{\mathrm{ramp}}}\right), \quad a_2=\frac{1}{RC}$$

Three roots of Equation (4) consist of a pair of conjugate complex ones and a real one. It can be known from Routh-Hurwitz stability criterion, that when $a_1a_2<a_0$ the system becomes unstable. The set of parameter values fulfilling the equality $a_1a_2=a_0$ corresponds to a low-frequency oscillation of the system. Indeed, $a_1a_2=a_0$ implies that the pair of conjugate roots is located at the imaginary axis of the complex plane ($s_{1,2}=\pm j\omega_{\mathrm{h}}$,). Therefore, from (4), we have,

$$a_0-a_2\omega_{\mathrm{h}}^2+j\omega_{\mathrm{h}}(a_1-\omega_{\mathrm{h}}^2)=0 \qquad (5)$$

Where, ω_{h} represents the critical oscillation angular frequency.

From Equation (5), we obtain,

$$\omega_{\mathrm{h}}=\sqrt{a_1}=\sqrt{a_0/a_2} \qquad (6)$$

In terms of the physical parameters of the system, the following equality at the boundary of stability is obtained from $a_1a_2=a_0$.

$$k_{\mathrm{p}}V_{\mathrm{g}}(RC-\tau)=\tau V_{\mathrm{ramp}} \qquad (7)$$

Equation (8) implies that high input voltage V_{g} and light load (large value of R) would result in a low-frequency oscillation, when the other system parameters keep constant.

3. Filter-Based perturbation control method

Figure 2 (a) shows the detailed information of the output voltage v_{o} in stable situation. It contains only two kinds of frequency components, the signal v_{b} with the same frequency with the sinusoidal reference and the switching signal v_{s}. However, in the case of a low-frequency oscillation, an oscillation frequency component v_h appears, as shown in **Figure** 2(b). Compared with the oscillation signal v_h, the amplitude of the switching ripple v_s is much small so as to be neglected in theoretical analysis.

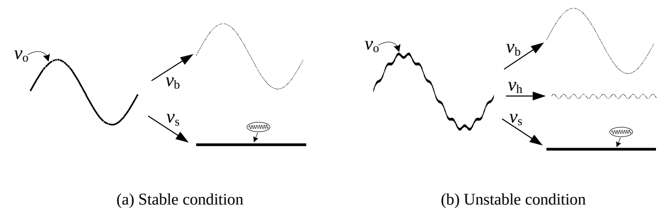

Figure 2. Decomposition of the output voltage waveform

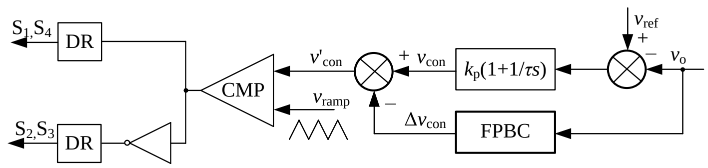

Figure 3. The control block diagram with FBPC

The whole control block diagram with FBPC is represented in **Figure 3**. Here, we will design FBPC in frequency domain and consider its transfer function as $G_s(j\omega)$. Our control target is that the perturbation control signal Δv_{con} of FBPC vanishes when the system is stable. Therefore, the following equations should be guaranteed.

$$\begin{cases} |\Delta v_{con}(j\omega_b)| = |V_o(j\omega_b)||G_s(j\omega_b)| \approx 0 \\ |\Delta v_{con}(j\omega_s)| = |V_o(j\omega_s)||G_s(j\omega_s)| \approx 0 \\ |\Delta v_{con}(0)| = |V_o(0)||G_s(0)| \approx 0 \\ |\Delta v_{con}(j\omega)| \neq 0, \omega \neq \omega_b, \omega \neq 0 \end{cases} \quad (8)$$

where ω_b and ω_s represent the reference angular frequency and switching angular frequency respectively.

For the voltage-mode inverter, the direct current (DC) component of the output voltage v_o closes to zero and its alternative current (AC) is a non-zero value. That is $V_o(0)=0$ and $V_o(j\omega_b)\neq 0$. Moreover, it can be concluded from above analysis that $V_o(j\omega_s)\approx 0$. Therefore, from Equation (8), we obtain,

$$\begin{cases} |G_s(j\omega_b)| = 0 \\ |G_s(j\omega)| \neq 0, \omega \neq \omega_b, \omega \neq 0 \end{cases} \quad (9)$$

From Equation (9), we will use a cascaded connection of a second order filter and a proportional controller to realize the FBPC controller $G_s(j\omega)$.

$$G_s(j\omega) = G_k(j\omega)G_f(j\omega) = p\frac{k_f(\omega_b^2 - \omega^2)}{j\frac{\omega_b}{Q}\omega + \omega_b^2 - \omega^2} = k_s\frac{(\omega_b^2 - \omega^2)}{j\frac{\omega_b}{Q}\omega + \omega_b^2 - \omega^2} \qquad (10)$$

where $G_k(j\omega)$ and $G_f(j\omega)$ represent the proportional controller and the second order filter, respectively. Here, p is the proportional gain, k_f is the DC gain of the second order filter, k_s is the total gain of FBPC and ω_c is the characteristic angular frequency. Q is the equivalent quality factor, defined by the following equation

$$Q = \frac{1}{2(2-k_f)} \qquad (11)$$

Figure 4 shows an implementation of FBPC with analog circuit. Some expressions are obtained as follows,

$$\omega_b = \frac{1}{RC}, k_f = 1 + \frac{R_b}{R_a}, p = \frac{R_f}{R_1}, k_s = pk_f \qquad (12)$$

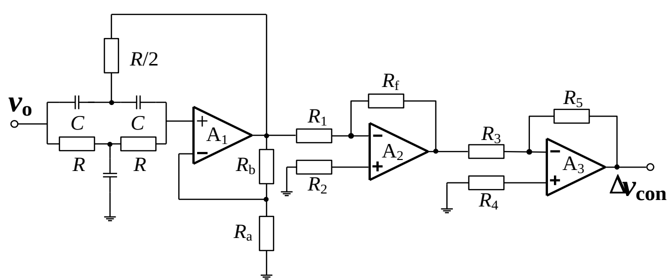

Figure 4. The analog circuit of FBPC

When FBPC is applied to the system, the new loop gain becomes

$$T'(s) = \frac{HG_{vd}(s)\left(G_c(s) + G_s(s)\right)}{V_{ramp}} \qquad (13)$$

The new closed-loop transfer function is,

$$F'(s) = \frac{1}{1+T'(s)} \qquad (14)$$

Hence, from Equation (14) the system stability with FBPC can be analyzed.

4. NUMERICAL SIMULATION AND EXPERIMENTAL VALIDATION

4.1 Extending the stability region with FBPC

The parameters values of the inverter system are shown in **Table 1**.

Table 1 Circuit and control parameters in simulation and experiment

Symbol	Name	Value
V_g	DC input voltage	20V
V_{ref}	Reference output voltage	8sin($\omega t+\varphi$)V
f_r	Reference voltage frequency	50Hz
L	Filter inductor	1.5mH
C	Filter capacitor	44μF
R	load	4.4~6.67Ω
f_s	Switching frequency	25kHz
V_{ramp}	Triangular Carrier	4V
ω_b	Filter angular frequency	100π rad/s
k_p	Proportional gain	0.3411
τ	Integral time constant	0.1463ms

Based on the Equations (7) and (14), the stability boundaries of the system with and without FBPC can be obtained in terms of the input voltage V_g and the load resistance R, respectively. The control parameters of FBPC were selected as k_s=2.1, k_f=1.05, p=2, $\omega_b=2\pi f_r$, f_r=50 Hz. The stability results are shown in **Figure 5**, from which it can be seen that the stability area of the system with FBPC becomes larger.

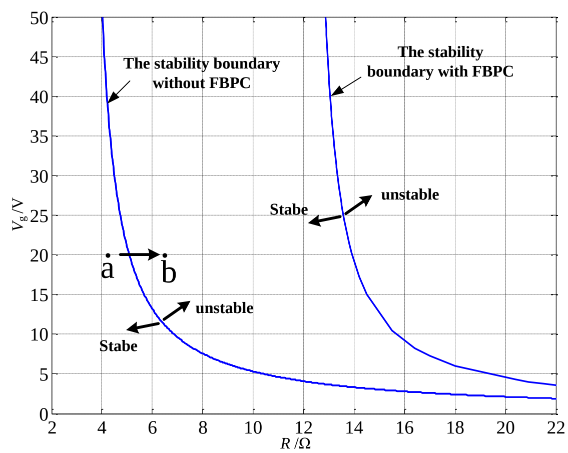

Figure 5. The stability boundaries of the system with and without FBPC

4.2 Simulation results

Figures 6(a)-(b) shows the simulation results of transient response of the output voltage v_o, the compensation signal v_{con} and the control signal Δv_{con} for a load step with R changing from 4.4Ω to 6.6Ω (from point a to point b in **Figure 5**). Without FBPC, the low-frequency oscillation occurs after a load step. Reversely, it maintains stable with FBPC.

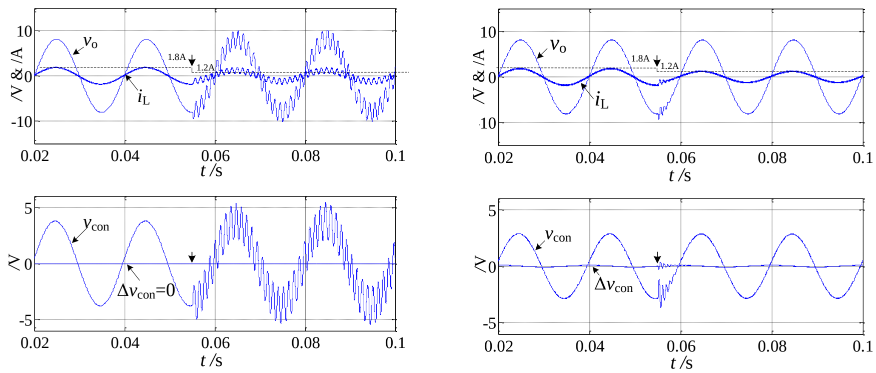

(a) (b)

Figure 6. Transient response for a load step from heavy load to light load, (a) Without FBPC, (b) With FBPC

4.3 Experimental verification

The photo of the laboratory prototype and the schematic diagram of the experiment circuit are shown in **Figures 7** (a) and (b), respectively. The MOSFET is SPW47N60C3 and its drive chip is IR2103. The control circuits are constructed with simple analog ICs and operational amplifiers, consisting of LF347, LM393, CD4049 and so on. The experiment parameters are basic consisted with Table 1.

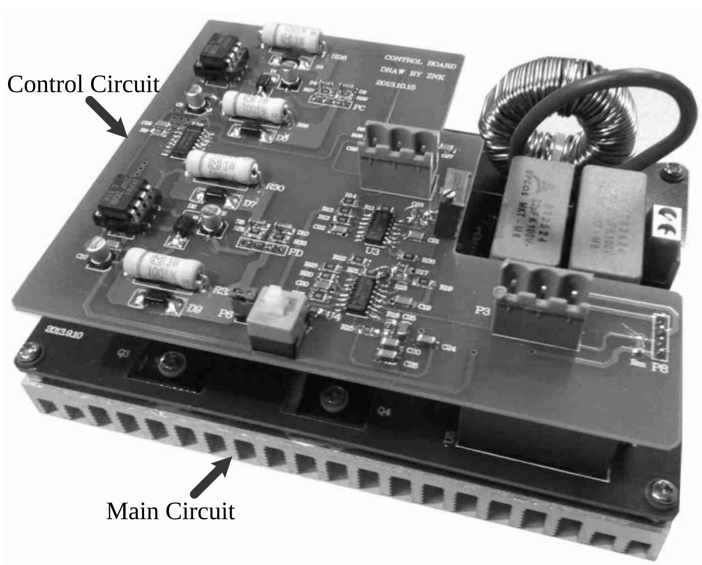

(a)

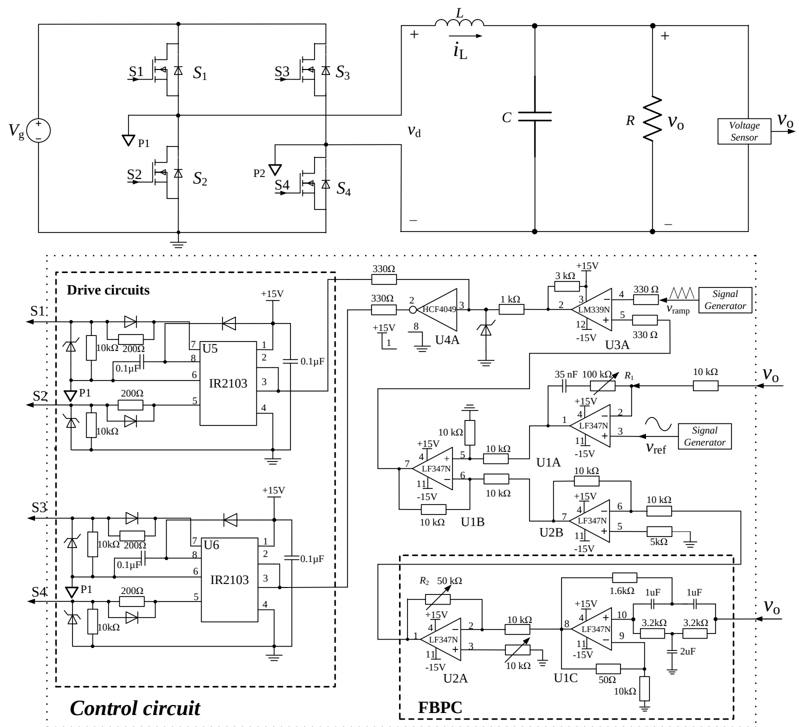

(b)

Figure 7. Experiment circuits (a) photo of the laboratory prototype, (b) schematic diagram of experiment circuits

Figure 8(a) shows the load transient response of the output voltage and the inductor current without FPBC. After the load current jumps from 1.8A to 1.2A, the oscillation occurs. From **Figure 8**(b), it can be seen that with FPBC, the system is controlled stable after a load step. That is to say, the proposed control can extend the stability region. Meanwhile, the total harmonic distortions (THD) of the output are largely reduced. Moreover, Δv_{con} is smaller than the compensator signal v_{con}. Therefore, it has a little impact of the FBPC on the system steady-state output performance.

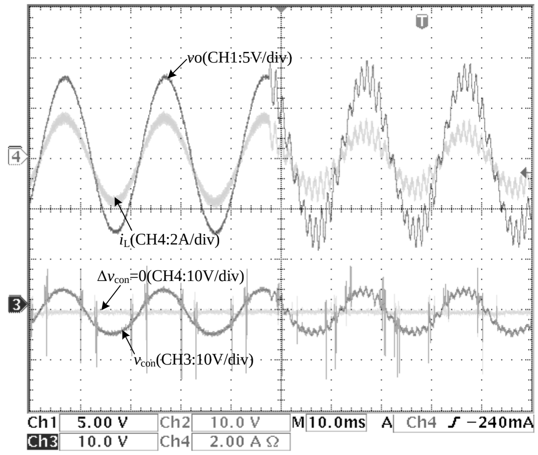

(a)

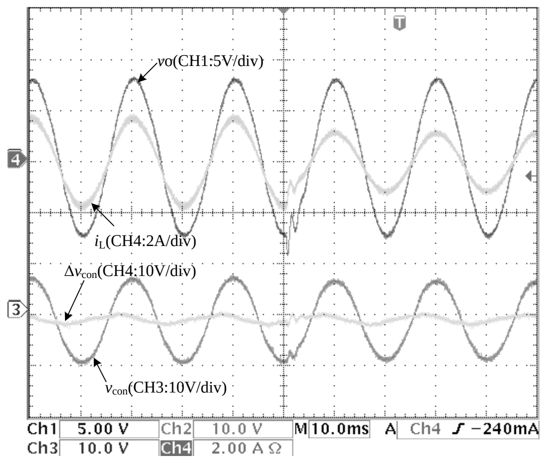

(b)

Figure 8. Experimental waveforms of the load transient, (a) Without FBPC, (b) With FBPC

5. CONCLUTIONS

A filter-based perturbation control method is proposed in this paper to suppress the low-frequency oscillation in voltage-mode H-bridge DC-AC inverter well. The numerical simulation and experimental results show that it has a good effect of the proposed FBPC on the system performances such as stability and THD and its implementation is simple. Furthermore, the control method is applicable to other types of switching power converters.

ACKNOWLEDGEMENTS

This work was supported by National Natural Science Foundation of China (Grant No. 51377185) and the Scientific Research Foundation of State Key Lab. of Power Transmission Equipment and System Security (2007DA10512711210).

REFERENCES

1. Yao ZL, Xiao L. Control of single-phase grid-connected inverters with nonlinear loads. *IEEE Transactions on Industrial Electronics* 2013, 60(4):1384-1389.
2. Zhao B, Song Q, Liu WH, Xiao Y. Next-generation multi-functional modular intelligent UPS system for smart grid. *IEEE Transactions on Industrial Electronics* 2013, 60(9):3602-3618.
3. Robert B, Robert C. Border collision bifurcations in a one-dimensional piecewise smooth map for a PWM current programmed H-bridge inverter. *International Journal of Control* 2002; 75(16):1356-1367.
4. Li M, Dai D, Ma XK. Slow-Scale and Fast-Scale Instabilities in Voltage-Mode Controlled Full-Bridge Inverter. *Circuits System Signal Process* 2008; 27:811.
5. El Aroudi A, Rodriguez E, Orabi M, Alarcon E. Modeling of switching frequency instabilities in buck-based DC–AC H-bridge inverters. *International Journal of Circuit Theory and Applications* 2011; 39:175-193.
6. Wu XL, Xiao GC, Lei B. Simplified discrete-time modeling for convenient stability prediction and digital control design. *IEEE Transactions on Power Electronics* 2013, 28(11):5333-5342.
7. Mazumder SK, Nayfeh AH, Boroyevich D. Theoretical and Experimental Investigation of the Fast- and Slow-Scale Instabilities of a DC–DC Converter. *IEEE Transactions Power Electronics* 2001, 16(2):201-216.
8. Iu HHC, Zhou YF, Tse CK. Fast-scale instability in a PFC boost converter under average current-mode control. *International Journal of Circuit Theory and Applications* 2003; 50(8):611-624.
9. Hamill DC, Deane JHB, Jefferies J. Modeling of Chaotic DC-DC Converters by Iterated Nonlinear Mappings. *IEEE Transactions on Power Electronics* 1992; 7(1):25-36.
10. Tsc CK. Flip Bifurcation and Chaos in Three-state Boost Switching Regulators. *IEEE Transactions on Circuits and Systems I* 1994; 41(1):6-23.
11. Deane JHB, Hamill DC. Improvement of power supply EMC by chaos. *Electronic Letter* 1996; 32(12): 1045.
12. Pyragas K. Continuous control of chaos by self-controlling feedback. *Physics Letter A* 1992; 170(6):421-428.

13. Iu HHC, Robert B. Control of Chaos in a PWM Current-Mode H-Bridge Inverter Using Time-Delayed Feedback. *IEEE Transactions. Circuits System I* 2003; 50(8): 1125-1129.
14. Robert B, Feki M, Iu HHC. Control of a PWM Inverter using Proportional plus Extended time-Delayed Feedback. *International Journal of Bifurcation and Chaos* 2006; 16(1):113-128.
15. El Aroudi A, Orabi M. Stabilizing Technique for AC–DC Boost PFC Converter Based on Time Delay Feedback. *IEEE Transactions Circuits Systems II* 2010; 57(3):56-60.
16. Wong SC, Wu X, Tse CK. Sustained slow-scale oscillation in higher order current-mode controlled converter. *IEEE Transactions on Circuits and Systems II: Express Briefs* 2008; 55(5): 489-493.
17. Wang FQ, Zhang H, Ma XK. Analysis of Slow-Scale Instability in Boost PFC Converter Using the Method of Harmonic Balance and Floquet Theory. *IEEE Transactions on Circuits and Systems I* 2010; 57(2):405-414.
18. Wan C, Huang M, Tse CK, Wong SC, Ruan XB. Nonlinear behavior and instability in three-phase boost rectifier connected to non-ideal power grid with interacting load. *IEEE Transactions on Power Electronics* 2013; 28(7):3255-3265.
19. El Aroudi A, Rodríguez E, Leyva R, Alarcón E. A Design-Oriented Combined Approach for Bifurcation Prediction in Switched-Mode Power Converters. *IEEE Transactions Circuits Systems II* 2010; 57(3):218-222.
20. Lu WG, Zhou LW, Luo QM, Zhang XF. Non-invasive chaos control of DC–DC converter and its optimization Filter based non-invasive control of chaos in Buck converter. *Physics Letter A* 2008; 372:3217-3222.
21. Lu WG, Zhou LW, Luo QM, Wu JK. Non-invasive chaos control of DC–DC converter and its optimization. *International Journal of Circuit Theory and Applications* 2011; 39:159-174.